ACADEMIA ROMÂNĂ
Revue Roumaine de Chimie
https://www.icf.ro/rrch/

Rev. Roum. Chim.,
2026, *71*(7–8), 477–482
DOI: 10.33224/rrch.2026.71.7-8.05

Dedicated to Professor Mihaela Hillebrand
on the occasion of her 85th anniversary

THERMAL DENATURATION OF SERUM ALBUMIN MEDIATED BY CAFFEIC ACID: FLUORESCENCE AND MICROCALORIMETRY INSIGHTS

Aurica PRECUPAS, Iulia MATEI* and Vlad T. POPA

"Ilie Murgulescu" Institute of Physical Chemistry of the Roumanian Academy,
202 Splaiul Independentei, 060021 Bucharest, Roumania

Received March 15, 2026

Properly folded proteins are essential for enzymatic activity, signal transduction, transport and cellular regulation. Thermal misfolding or unfolding can disrupt these functions, leading to aggregation, loss of activity or disease. In this study, the effect of caffeic acid (CA) on the thermal denaturation of bovine serum albumin (BSA) was assessed using differential scanning microcalorimetry (μDSC) and steady-state fluorescence spectroscopy. Microcalorimetric results demonstrated that CA increases the apparent thermal stability of BSA, highlighting the role of polyphenols in modulating protein denaturation pathways. Fluorescence data provided additional information on microenvironmental changes around the emissive residues occurring prior to global unfolding. The collective results emphasize the importance of synergistic methodologies for a comprehensive understanding of thermally-induced structural modifications in proteins in the presence of polyphenols.

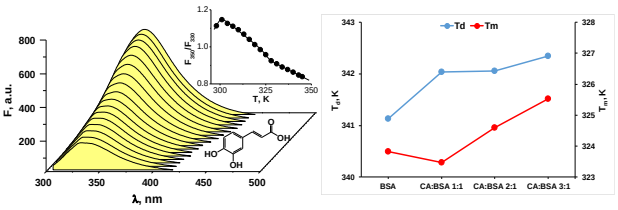

INTRODUCTION

The three-dimensional folding of proteins is essential for their biological function. Heat-induced stress causes proteins to unfold, by perturbing hydrogen-bonding networks and exposing hydrophobic residues. Partially unfolded proteins are prone to intermolecular interactions that lead to aggregation and to amyloid fibril formation, key mechanisms that underlie the pathogenesis of neurodegenerative disorders like systemic amyloidosis, Alzheimer's or Parkinson's diseases.[1] Understanding the molecular mechanisms of protein denaturation and aggregation is therefore critical for developing strategies to modulate and ultimately prevent amyloid formation.

The unfolding kinetics and thermal stability of proteins are known to be strongly influenced by the presence of exogeneous ligands.[2,3] Among them, polyphenols can significantly modulate the thermal stability of proteins through non-covalent interactions. Recent research has demonstrated that resveratrol binding to α-lactalbumin increases the denaturation temperature of the protein, thereby

* Corresponding author: iuliamatei@icf.ro

enhancing its thermal stability.[4] Tea polyphenols stabilize the conformation of soymilk protein upon heating, by increasing the α-helix content,[5] while quercetin stabilizes bovine serum albumin (BSA) against amyloid formation.[6] Caffeic acid (CA), a hydroxycinnamic acid with demonstrated neuroprotective activity,[7] has also been shown to interact with α-lactalbumin,[8] bovine β-lactoglobulin[9] and casein,[10] modulating the proteins' structural stability and thermal behaviour.

In this study, we investigate the effect of different concentrations of CA on the thermal denaturation of BSA by means of two complementary techniques, differential scanning microcalorimetry (μDSC) and steady-state fluorescence spectroscopy. μDSC directly measures the heat absorbed during protein unfolding, providing global thermodynamic parameters that reflect the cooperative unfolding of the protein's overall structure. Conversely, fluorescence spectroscopy monitors temperature-induced changes in the microenvironment of the emissive amino acid residues, specifically tryptophan (Trp), revealing local conformational rearrangements that occur prior to global unfolding. Together, these techniques enable a more complete understanding of the thermal denaturation of BSA in the presence of CA, by correlating site-specific structural perturbations with global thermodynamic stability.

RESULTS AND DISCUSSION

Thermodynamic stability and global structural change

Thermal denaturation of BSA is a sequential process characterized by structural unfolding of its three homologous domains (I, II and III) that possess different thermal stability.[11] The DSC thermogram for BSA in the absence of the CA ligand is presented in Fig. 1. It displays a main endothermic peak with a shoulder, consistent with previous reports that attribute this feature to the sequential unfolding of multiple structural domains: (i) the low temperature transition corresponds to the collapse of the N-terminal domain of BSA (domain I, in which Trp134 resides), the structural changes also affecting the vicinity of the Trp213 residue; (ii) the high temperature transition corresponds to the cooperative unfolding of the more compact domains II and III.[12,13]

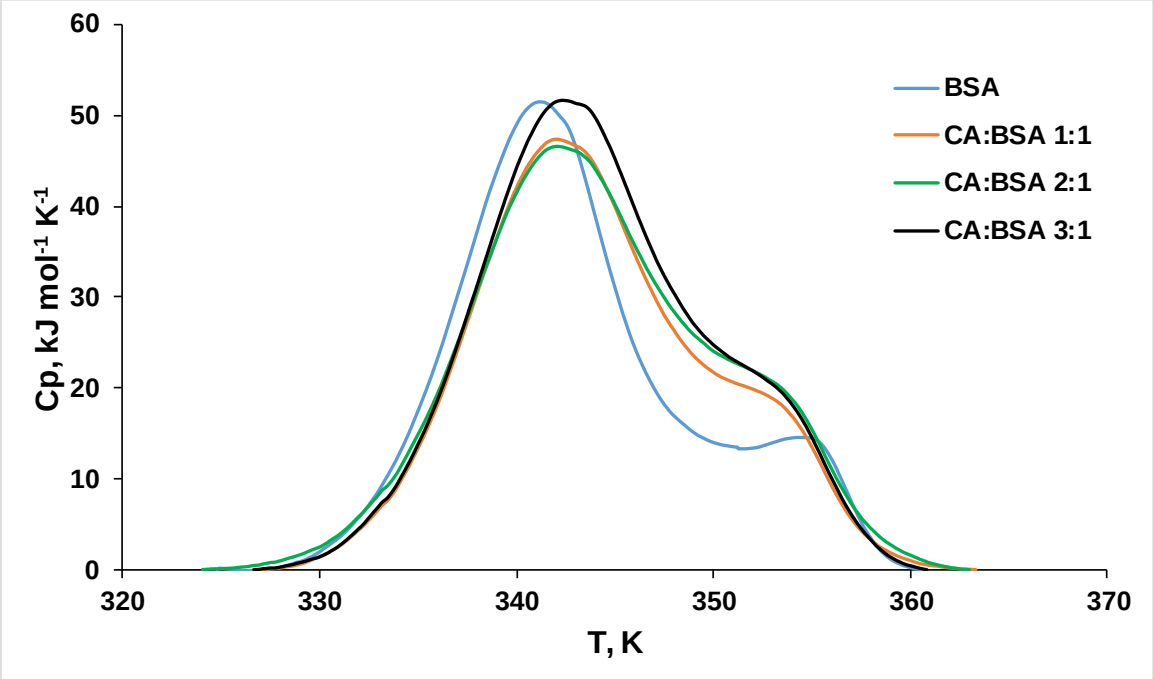

Fig. 1 – The μDSC scans of BSA (10^{-4} M) thermal denaturation in phosphate buffer NaH_2PO_4/Na_2HPO_4, 20 mM, pH 7.2, in the absence and in the presence of different CA concentrations.

The influence of different CA concentrations on the thermal denaturation of BSA is also presented in Fig. 1, and the denaturation parameters of BSA (denaturation temperature, T_d, and denaturation enthalpy change, ΔH) in the investigated systems are given in Fig. 2.

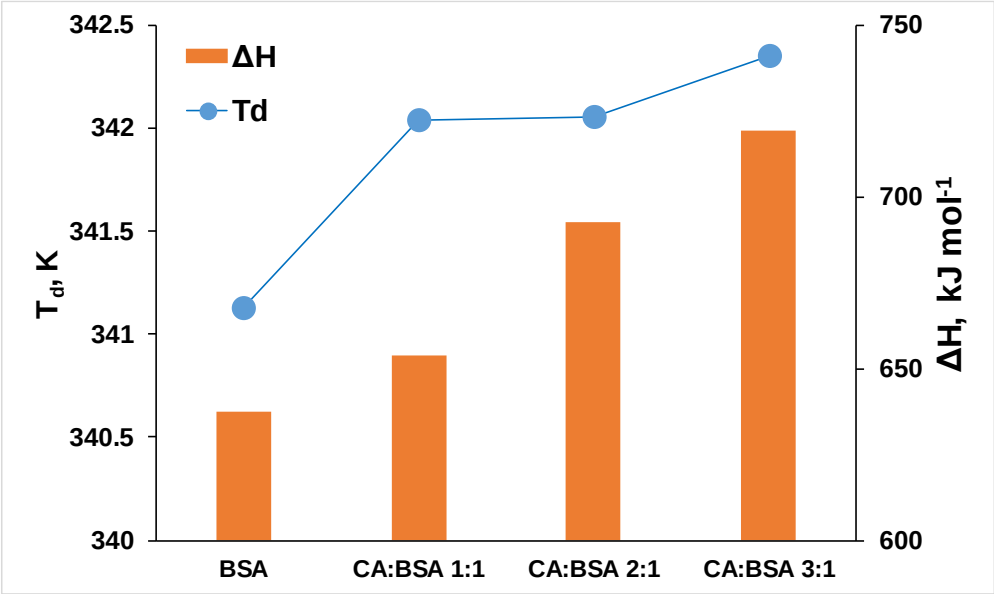

Fig. 2 – Thermodynamic parameters (T_d and ΔH) for BSA denaturation in the interacting systems.

It can be observed from Fig. 1 that the presence of CA shifts the peak maximum to higher temperature values, and the shoulder position to lower values. The increase in the T_d value with increasing CA concentration points to a clear stabilizing effect of the polyphenol on the native structure of BSA. Concurrently, higher ΔH values are obtained with increasing CA concentration, suggesting that unfolding becomes more energetically demanding, consistent with stronger stabilizing interactions and/or altered hydration of the protein–ligand complex. This suggests that CA stabilizes specific domains or intermediate conformations, enhancing the cooperativity of unfolding.

The μDSC results are in line with the known domain-specific binding behavior of BSA, and suggest that polyphenols like CA can modulate both the global and the local protein stability, potentially preventing early aggregation events during thermal stress. Similar effects have been identified for other phenolic compounds, including sinapic acid,[14] a structurally-related hydroxycinnamic acid derivative. The results are consistent with the previously reported CA-mediated stabilization of BSA observed using a different experimental setting: phosphate buffer KH_2PO_4/Na_2HPO_4, 100 mM, pH 7.4, and higher CA:BSA molar ratios of 3.5:1 and 20:1.[13] In this case, the stabilization of the BSA structure was attributed to CA binding at two different sites within subdomains IIA and IIIA, reinforcing the native fold and enhancing thermal resistance.

Conformational changes in the local microenvironment

Additional insight into temperature-induced local conformational changes in BSA, in the presence of CA, can be obtained by monitoring the intrinsic emission of Trp residues. Upon excitation at 295 nm, the large increase in the dipole moment of the indole group of Trp leads to an excited state that is highly sensitive to microenvironmental alterations, as reflected by changes in the intensity and/or position of the fluorescence band.[15] Native BSA contains two Trp residues, Trp134 and Trp213. While Trp134 is solvent-exposed, located near the protein surface at the interface of subdomains IA and IB, Trp213 is buried within a hydrophobic pocket in subdomain IIA, at the interface with subdomains IIB, IIIA and IB.[16] Importantly, this pocket is one of the two binding sites identified for CA.[13] During thermal denaturation, Trp134 and Trp213 generally reflect early-stage and late-stage conformational changes, respectively.[17]

Fig. 3 shows the fluorescence spectra of BSA recorded during heating in the temperature range 298–345 K, in the absence and in the presence of CA (exemplified in Fig. 3B for the system CA:BSA 3:1). The quenching effect likely reflects CA binding in the vicinity of Trp213, consistent with previously proposed binding in subdomain IIA.

The hypsochromic shift (~8 nm) of the fluorescence band upon heating can be rationalized

in terms of the average Trp environment becoming more shielded from the solvent.[18] A similar behaviour was reported for α-amylase from pig pancreas[19] and for an IgG monoclonal antibody.[20]

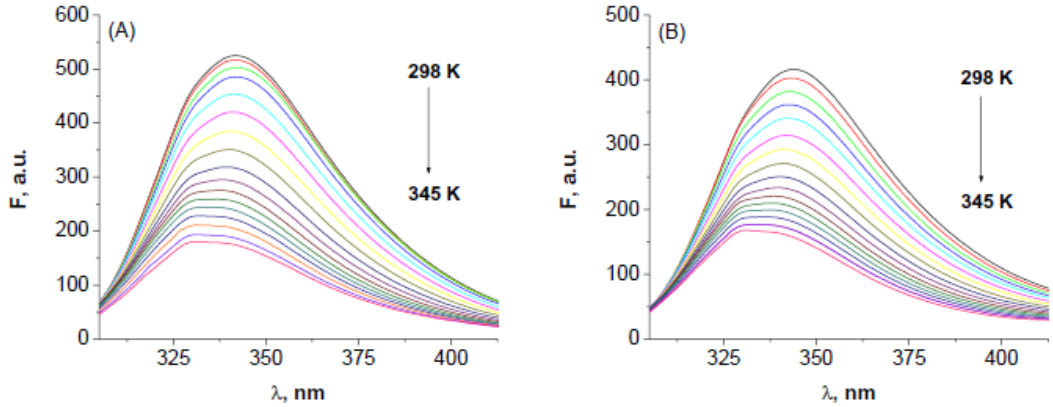

Fig. 3 – Fluorescence spectra of BSA (3×10^{-6} M) in the absence (A) and in the presence of CA at CA:BSA molar ratio of 3:1 (B), during heating.

For thermally-induced conformational transitions, the fluorescence data can be analysed considering a simple two-state model describing the transition from the native state to the unfolded state.[21] A typical temperature-dependent plot of $y(T)$, the spectral parameter sensitive to unfolding (*vide infra*), follows the sigmoidal two-state transition described by equation 1:[22,23]

$$y(T) = \frac{(y_f + m_f T) + (y_u + m_u T)\cdot e^{\frac{-\Delta G(T)}{RT}}}{1 + e^{\frac{-\Delta G(T)}{RT}}} \quad (1)$$

where y_f and m_f, and y_u and m_u, are the slopes and intercepts of the pre-transition (maximally populated folded state) and post-transition (maximally populated unfolded state) baselines, respectively. These baselines account for minor rearrangements of structure and/or solvent at the initial and final unfolding stages. ΔG(T) is the Gibbs free energy difference between the unfolded and folded (native) states, R is the gas constant and T is the absolute temperature. In equation 1, ΔG is expressed by the modified Gibbs-Helmholtz equation 2:[24]

$$\Delta G(T) = \Delta H_m\left(1 - \frac{T}{T_m}\right) - \Delta C_P\left[(T_m - T) + T\ln\frac{T}{T_m}\right] \quad (2)$$

T_m represents the melting temperature, or midpoint transition temperature, defined as the temperature at which the folded and unfolded states are equally populated. ΔH_m represents the enthalpy change upon unfolding at T_m. ΔC_P is the difference in heat capacity between the unfolded and native states.

Parameters y_f, m_f, y_u, m_u, T_m and ΔH_m can be estimated by non-linear least-squares analysis[25] of the thermal denaturation curves using equation 1 in which ΔG(T) is replaced by the Gibbs-Helmholtz expression. The ΔC_P value of each system is considered to not vary significantly over the investigated temperature range[26-28] and, as recommended in literature,[23,24,29] is taken from the μDSC measurements (Table 1) and introduced as a constant in each fitting.

The spectral parameter $y(T)$ selected for data analysis is the ratio of the fluorescence intensities at 350 nm (ascribed to solvent-exposed Trp residues) and at 330 nm (reporting on Trp residues within hydrophobic pockets), denoted F_{350}/F_{330}.[30,31] For most protein systems, ratiometric analysis provides a more reliable estimation of the T_m value compared to the use of the fluorescence intensity at a singular wavelength.[32] The use of F_{350}/F_{330} removes the background thermal quenching that arises from collisions with solvent molecules and neighbouring amino acid residues, which is most apparent in the pre- and post-transition baselines but can also mask or distort the specific signal of protein unfolding. Since the temperature-dependence of fluorescence affects both wavelengths equally, F_{350}/F_{330} also corrects for scattering and inner filter effects, and instrumental fluctuations.

The thermal denaturation curves for the systems under investigation are depicted in Fig. 4, and the extracted values of T_m and ΔH_m are listed in Table 1. It can be observed that the variation trends in T_m and ΔH_m are similar to those in T_d and ΔH. The stabilizing effect of the CA polyphenol on the native structure of BSA is most evident for the CA:BSA 3:1 system. Compared to μDSC, the fluorescence measurements report overall lower T_m and ΔH_m values. The denaturation temperature might

increase slightly with the BSA concentration,[11] which is higher for calorimetric measurements due to limitations in each technique. Nevertheless, the lower T_m values obtained by fluorescence are representative of a loosening in the BSA tertiary structure (in specific domains/side chains in the vicinity of Trp residues) that occurs prior to the global structural collapse.

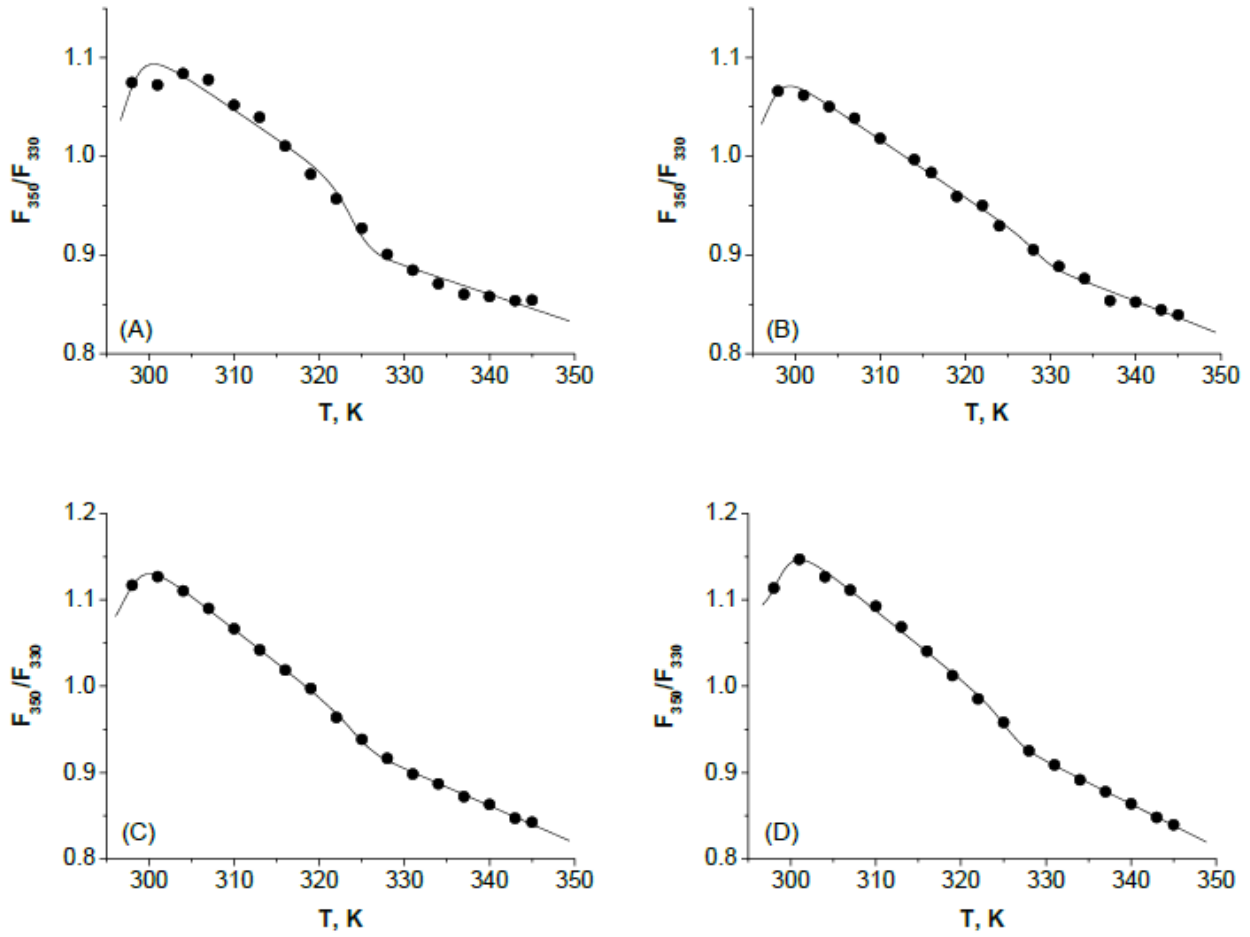

Fig. 4 – Fluorescence intensity ratio, F_{350}/F_{330}, as a function of temperature for (A) BSA, (B) CA:BSA 1:1, (C) CA:BSA 2:1 and (D) CA:BSA 3:1 systems. Continuous lines represent fits according to equation 1.

Table 1

Thermodynamic parameters of BSA as a function of CA concentration

System	T_m (K)	ΔH_m (kJ mol^{-1})	ΔCp (kJ mol^{-1} K^{-1})	T_d (K)	ΔH (kJ mol^{-1})
BSA	323.83	703.39	51.52	341.13	637.55
CA:BSA 1:1	323.47	646.60	47.40	342.04	653.77
CA:BSA 2:1	324.60	654.29	46.61	342.06	692.73
CA:BSA 3:1	325.52	717.06	51.68	342.35	719.56

Note: The T_m and ΔH_m values are derived from fluorescence measurements, while the ΔC_P, T_d and ΔH values are derived from μDSC measurements.

EXPERIMENTAL

Caffeic acid and bovine serum albumin (≥98%, fatty acid free) were acquired from Sigma-Aldrich. BSA solutions (10^{-4} M for μDSC measurements and 3×10^{-6} M for fluorescence measurements) were prepared in phosphate buffer (NaH_2PO_4/Na_2HPO_4) 20 mM, pH 7.2, in the absence and in the presence of CA concentrations in the range 0–3×10^{-4} M (CA:BSA molar ratios of 1:1, 2:1 and 3:1).

The μDSC measurements were carried out using a μDSC7 evo calorimeter (Setaram). Samples were heated from 298 to 363 K at a scan rate of 1 K min^{-1}. Data acquisition and analysis were performed using the Calisto v1.077 software, applying a sigmoid baseline. The obtained endothermic peak

corresponds to the typical two-state thermally induced protein denaturation following the Lumry-Eyring model.[21] The denaturation parameters were determined by analysing the endothermic peak: the point where maximum heat is absorbed during the unfolding process (the denaturation temperature, T_d), and the area under this peak, when integrated (the denaturation enthalpy change, ΔH). The per mol quantities were calculated taking into account the sample volume and the protein concentration.

Fluorescence measurements were performed on a JASCO FP-8250 spectrofluorometer. An excitation wavelength of 295 nm was used to specifically excite tryptophan and minimize interference from the other emissive amino acids, tyrosine and phenylalanine. Emission spectra were recorded in the temperature range 298–345 K with a 3 K step after an equilibration period of 5 min at each temperature. The spectra were corrected for the inner filter effect of CA according to the procedure described in literature.[33]

CONCLUSIONS

In this study, μDSC and fluorescence spectroscopy have been applied to investigate the thermal denaturation of BSA in the presence of the polyphenol CA. The fluorometric method has been previously used in conjunction with μDSC to estimate phase transitions in pluronic/polysaccharide gelling systems.[34] Here, the two methods provide complementary information on the effect of CA on thermally-induced global and local structural changes in BSA. The findings highlight the ability of the polyphenol to modulate protein stability through site-specific interactions, and suggest broader applications in protein preservation and aggregation prevention.

Acknowledgements. This work was supported by a grant of the Ministry of Research, Innovation and Digitization, CNCS-UEFISCDI, contract number 93TE/03.01.2025, project code PN-IV-P2-2.1-TE-2023-0189, within PNCDI IV. It was carried out within the research project "Nonuniform bio-binding" of the "Ilie Murgulescu" Institute of Physical Chemistry of the Roumanian Academy.

REFERENCES

1. D. J. Rinauro, F. Chiti, M. Vendruscolo and R. Limbocker, *Mol. Neurodegeneration*, **2024**, *19*, 20.
2. J. F. Brandts and L. N. Lin, *Biochemistry*, **1990**, *29*, 6927–6940.
3. P. Cimmperman, L. Baranauskienė, S. Jachimovičiūtė, J. Jachno, J. Torresan, V. Michailovienė, J. Matulienė, J. Sereikaitė, V. Bumelis and D. Matulis, *Biophys. J.*, **2008**, *95*, 3222–3231.
4. A. Precupas, D. Gheorghe, A. R. Leonties and V. T. Popa, *Biomedicines*, **2024**, *12*, 2176.
5. G. Ge, W. Guo, J. Zheng, M. Zhao and W. Sun, *Food Hydrocoll.*, **2021**, *111*, 106177.
6. A. G. Rathod, P. Tiwari, J. Shaily and S. Tiwari, *Colloids Surf. B*, **2025**, 252, 114663.
7. M. Alam, S. Ahmed, A. M. Elasbali, M. Adnan, S. Alam, M. I. Hassan and V. R. Pasupuleti, *Front. Oncol.*, **2022**, *12*, 860508.
8. N. A. Al-Shabib, J. M. Khan, A. M. Al-Amri, A. Malik, F. M. Husain, P. Sharma, A. Emerson, V. Kumar and P. Sen, *ACS Omega*, **2023**, *8*, 19853–19861.
9. N. Stănciuc, G. Râpeanu, G. E. Bahrim and I. Aprodu, *Biomolecules*, **2020**, *10*, 1096.
10. S. Shen, H. Yang, X. Liu, D. Tang and J. Cheng, *LWT*, **2023**, *186*, 115199.
11. A. Michnik, *J. Therm. Anal. Cal.* **2003**, *71*, 509–519.
12. A. Precupas, R. Sandu and V. T. Popa, *J. Phys. Chem. B*, **2016**, *120*, 9362–9375.
13. A. Precupas, R. Sandu, A. R. Leonties, D. F. Anghel and V. T. Popa, *New J. Chem.*, **2017**, *41*, 15003–15015.
14. A. Precupas and V. T. Popa, *Int. J. Mol. Sci.*, **2024**, *25*, 936.
15. F. H. dos Santos Rodrigues, G. Garcia Delgado, T. Santana da Costa and L. Tasic, *BBA Advances*, **2023**, *3*, 100091.
16. K. A. Majorek, P. J. Porebski, A. Dayal, M. D. Zimmerman, K. Jablonska, A. J. Stewart, M. Chruszcz and W. Minor, *Mol. Immunol.*, **2012**, *52*, 174–182.
17. Y. C. Chou, T. Y. Lin and M. Y. Tsai, *J. Chin. Chem. Soc.*, **2023**, *70*, 386–393.
18. M. S. Celej, G. G. Montich and G. D. Fidelio, *Protein Sci.*, **2003**, *12*, 1496–1506.
19. C. Duy and J. Fitter, *Biophys. J.*, **2006**, *90*, 3704–3711.
20. M. L. Brader, T. Estey, S. Bai, R. W. Alston, K. K. Lucas, S. Lantz, P. Landsman and K. M. Maloney, *Mol. Pharmaceutics*, **2015**, *12*, 1005–1017.
21. J. M. Sanchez-Ruiz, *Biophys. J.*, **1992**, *61*, 921–935.
22. K. Saini and S. Deep, *Eur. Biophys. J.*, **2010**, *39*, 1445–1451.
23. C. N. Pace, *Trends Biotechnol.*, **1990**, *8*, 93–98.
24. C. N. Pace, B. A. Shirley and J. A. Thomson, "Measuring the conformational stability of a protein" in "Protein Structure: A Practical Approach", T. Creighton (Ed.), IRL Press, New York, 1997, 311–330.
25. M. R. Eftink, *Biophys. J.*, **1994**, *66*, 482–501.
26. M. Winiewska-Szajewska and J. Poznański, *Biophys. Rev.*, **2025**, *17*, 199–223.
27. C. N. Pace and D. V. Laurents, *Biochemistry*, **1989**, *28*, 2520-2525.
28. W. J. Becktel and J. A. Schellman, *Biopolymers*, **1987**, *26*, 1859–1877.
29. B. Ibarra-Molero and J. M. Sanchez-Ruiz, *Biochemistry*, **1996**, *35*, 14689–14702.
30. Y. K. Reshetnyak and E. A. Burstein, *Biophys. J.*, **2001**, *81*, 1710–1734.
31. M. Weichel, S. Bassarab and P. Garidel, *BioProcess Int.*, **2008**, *6*, 42–52.
32. K. K. Turoverov, S. Yu. Haitlina and G. P. Pinaev, *FEBS Lett.*, **1976**, *62*, 4–6.
33. D. E. Epps, T. J. Raub, V. Caiolfa, A. Chiari and M. Zamai, *J. Pharm. Pharmacol.*, **1999**, *51*, 41–48.
34. G. A. Balan, A. Precupas and I. Matei, *Gels*, **2023**, *9*, 939.